# Thermographical Analysis of Turbo-generator Rotor

A. N. Singh*, W. Doorsamy**, W. Cronje*

*University of the Witwatersrand, Johannesburg, South Africa

**University of Johannesburg, Johannesburg, South Africa

**Abstract**

Refurbished or newly constructed utility-scale turbo-generator rotors requires stringent acceptance testing before commissioning and subsequent operation thereof. Conventional methods of testing are inadequate in detecting and locating thermally induced problems. This paper presents a thermographic method for carrying out thermal instability testing of generator rotors. An experimental setup is used to map the thermal distribution of the generator rotor. Implementation and testing of the method is carried out in a laboratory setting using a down-scaled turbo-generator rotor.

*Keywords:* *Turbo-generator rotor; thermographical analysis; thermal instability testing.*

## 1. Introduction

Modern large turbo-generator rotors are predisposed to thermal sensitivity owing to their complex design, material composition and operating requirements. Manufacturing and refurbishment techniques introduce component variations which cause most rotors to exhibit some level of thermal sensitivity [1, 2]. Thermally induced vibration in generator rotors is by far the most difficult problem to diagnose and correct. Symptoms may be a bowed shaft and a vibration signature linked to the excitation current, but the possible underlying causes are numerous. It is especially difficult to physically determine mechanically dynamic or electrical causes of the thermal imbalance without excitation. A thorough inspection and methodical overhaul of the rotor in search of

anomalies will require the rotor to be separated from the stator. Since the exact conditions that cause the thermal unbalance are not acting on the rotor, physically identifying the anomaly is impracticable. This phenomenon is commonly referred to as thermal instability/sensitivity. Conventional balancing techniques and acceptance tests are not suited to detect and correct such problems [3].

This paper presents a method for detecting thermal instabilities on newly built and refurbished rotors using thermographic analysis. Through directly mapping the thermal distribution of the surface of generator rotor, the method offers the possibility of localising the root causes of existing instabilities. The initial concept and preliminary results of the direct thermal mapping of a turbo-generator rotor was first presented in [4]. The presented research build on this with substantial improvements to technique, and gives detailed description of the methodology together with results obtained from implementation and testing in a laboratory setting.

## 2. Contemporary Thermal analysis of Generator Rotors

Electrically induced unbalance typically manifests from the thermal behaviour of the rotor. As the rotor is excited by an increasing current, the copper winding will rise in temperature. The increasing temperature naturally causes the copper to expand within the slots and overhang area, but not in proportion to the expansion of the steel rotor forging, as the coefficient of expansion of copper is nearly twice that of steel. The expanding copper will exert axial forces on the other components of the rotor – slot contents, body wedges, blocking and coil retaining ring assembly [5]. The heat generated within the winding will also be conducted through the steel body and dissipated by the cooling medium. If this heat transfer process continues symmetrically along the body of the rotor, a thermal unbalance will not be experienced. However, if the heat transfer process or coil forces occur asymmetrically, an unbalance will be experienced, resulting in the bowing of the rotor body. The severity of the thermal bow will determine the amplitude of the vibration experienced at the bearings [6]. If the vibration levels exceed the operating limits of the rotor, this can result in failure and the loss of generating capacity.

Thermal Instability Testing (TIT) is common practice for major utilities and is performed at specially designed balancing facilities or in situ to determine the thermal behaviour of rotors [7]. TIT is generally performed after any major refurbishment work which has been conducted on the rotor i.e. rewind, slot liner replacements, major overhaul, retaining ring replacement etc. [8]. Two main testing methods are used worldwide: 1) Direct current injection into the rotor winding -i.e. Current thermal instability testing (CTIT) and, 2) Windage or friction heating - i.e. Friction thermal instability testing (FTIT). Different utilities prefer specific tests based on their own propriety experiences. The variations in methodology and lack of published data supporting either of the aforementioned tests create uncertainty as to which test is able to best detect any latent thermal imbalances within the rotor assembly.

The detection of rotor thermal sensitivity does not rely on any thermal characteristics measured during testing but rather on vibration monitoring. A thermal bow associated with thermal sensitivity is detected via vibration data. Vibration data analysis is currently the most widely used method for detecting problems with turbo-generator rotors [9], however it does not directly assist with locating the problem area. Solutions to the problem generally involve a compromise balance for minor imbalances or a full strip down for fault detection and repair for a major imbalance. Typical test procedures do not adequately consider thermal characteristics of the rotor. Rotor winding temperature may be determined using the following formula:

$$T_{Hot} = \Big[\Big(\frac{R_{Hot}}{R_{Cold}}\Big)(234.5 + T_{Cold})\Big] - 234.5 \tag{1}$$

where:

$T_{Cold}$ = reference temperature value,
$R_{Cold}$ = winding resistance at the reference temperature,
$R_{Hot}$ = winding resistance at the testing point, and
$234.5$ = thermal conductivity of copper.

In solving this equation, it is necessary to be aware of sources of uncertainty. Uncertainty can be categorised as either epistemic or aleatory [10]. Aleatoric uncertainty is characterised by the lack of predictability or intrinsic randomness of a phenomenon;

epistemic uncertainty is characterised by a deficit of knowledge. This approach requires that resistance and physical temperature measurements be known at a specific current and voltage level to obtain a reference value. Subsequent temperature rises can be calculated by utilising the rotor resistance measurement. The resistance measurement needs to be accurate and can be significantly affected by inaccuracies and errors in voltage and current readings [11]. This form of temperature monitoring is relatively basic, as it does not account for hot spots within the winding but rather the average rotor winding temperature. Furthermore, this method does not indicate the temperature of the rotor's other extremities such as the shaft, coil retaining rings, or rotor surface [12]. The uneven thermal profiles of all of these components can lead to thermal instability. This drawback undermines the reliability of this model as a means to determine rotor thermal characteristics. It best serves to indicate average temperature while performing TIT. Epistemic uncertainty is a feature of modelling methods such as presented in [13], which arises due to the simplifying assumptions required for constructing a model of a complex turbo-generator rotor. Accurately determining the thermal characteristics of the entire generator rotor body would be invaluable in determining the differences between FTIT and CTIT through a more practical method that is not influenced by epistemic uncertainty.

## 3. Use of Infrared (IR) Sensors

The shortcomings of contemporary methods for thermal analysis of turbo-generator rotors must be overcome to improve acceptance testing processes. Rotor telemetry systems have been devised to monitor rotor ground faults and temperature measurement and have improved significantly over the past decade. Temperatures are monitored by installing resistance temperature detectors (RTDs) within the rotor winding slots and under the coil retaining rings. The connections are wired to an antenna mounted on the rotor body. The antenna transmits the digitised temperature values to a data acquisition unit external to the generator [14]. This method is dependent on the number of RTDs installed for accurate measurement of the thermal distribution of the rotor. Hot spot detection may still be a challenge depending on the RTD layout. Furthermore, this

method requires significant modifications to the rotor insulation system to facilitate the installation of the RTDs and routing of the connections, which will involve substantial rotor disassembly. The invasive nature of the process would lead to further design variations that could affect rotor operation and thermal performance. Therefore, this method of temperature detection is ruled out for the experimental setup.

The widespread use of infrared thermography within the electrical industry has been commonplace for a number of years [15, 16, 17, 18]. This non-contact, non-invasive method produces reliable and accurate results for fault finding and trouble shooting. Temperature measurements are made possible by detecting the radiant flux of an object; a temperature output is calculated through a calibration algorithm. Also referred to as a radiation thermometer, many varieties are available on the market today, from thermal imaging cameras to singular probes. Devices are able to measure a wide variety of temperature ranges and can operate at high speeds, making this approach an ideal choice for the proposed approach [19].

## 4. Thermal Mapping

The presented method of data capture is in the form of a matrix of temperature values corresponding to the physical mapping of the surface of the generator rotor. This method transforms these temperature measurements and physical coordinates into a 2-D heat map. Simply put, the direct thermal mapping method present the 3-D temperature data (of the rotor surface) as a 2-D heat map. A heat map consists of a number of rectangular rows (angular position) and columns (axial length) that represent data values against a colour scale (temperature). This is a widely used method to display large matrices within many different fields such as natural sciences and biological science [20, 21]. The experimental setup is able to capture surface temperature measurements together with physical coordinates that is used to create a heat map for easy interpretation and analysis of the thermal behaviour of the rotor under different thermal instability tests such as FTIT and CTIT. Furthermore, the rotor surface temperature map assists with root cause analysis and fault finding because it can be used to physically locate irregularities on the rotor.

### 4.1. Data Capturing

Data acquisition is facilitated via two streams. The data from the IR camera and proximity probe interface is captured via a data-acquisition unit linked to a computer utilising proprietary software from the IR camera manufacturer known as Optris PI Connect. The winding, ambient, and enclosure temperatures are captured via a separate unit linked to a computer. All data is time stamped to facilitate data synchronisation. An overview of the experimental layout and data acquisition is shown in fig. 1.

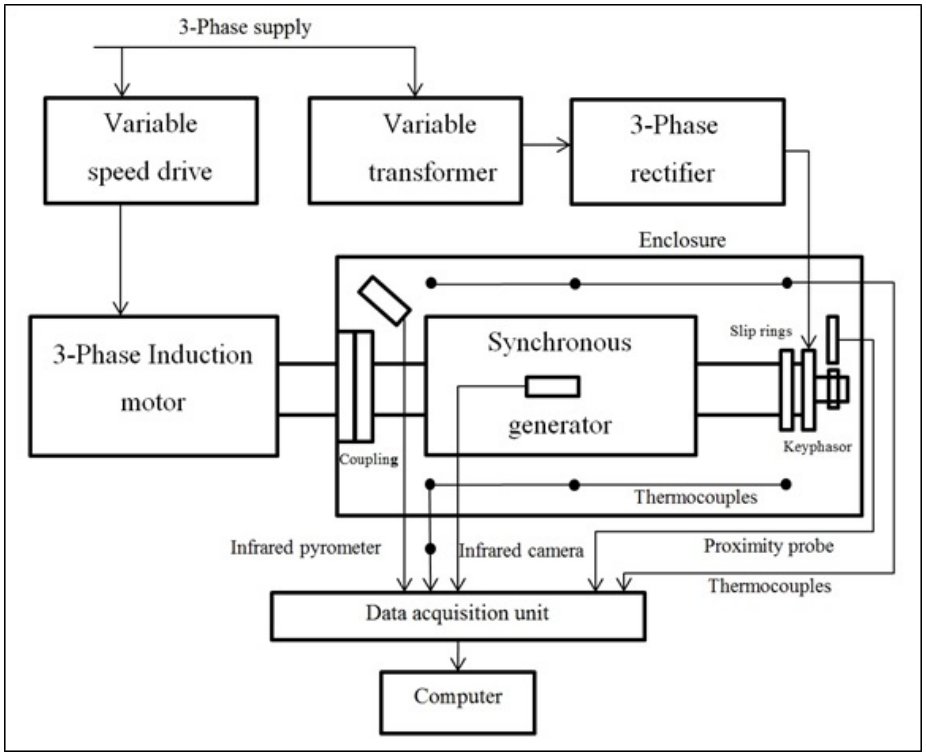


Figure 1: Experimental layout with associated instrumentation to capture the thermal profile of the rotor

### 4.2. Generating a Thermal Map of the Rotor

The initial step in constructing the heat map is to define the IR camera resolution pixel size that will correspond to the physical portion of the rotor to be measured. The distance of the IR camera from the test object (rotor) determines the size of the measurement pixel and therefore the map resolution. The further away the IR camera

is from the test object, the larger the pixel size. The pixel size is also dependant on the optical lens fitted to the IR Camera.

A 20 kVA mini-rotor (shown in fig. 2) designed to mimic a 600 MW turbo-generator rotor is used for validation and testing of the presented thermal mapping method (constructional details given in table 1). A keyphasor probe is also utilised to determine the angular position of the mini-rotor. This is achieved with the aid of a fixed collar with a machined notch and a proximity probe. An output is received when the notch passes the proximity probe and indicates when one revolution has passed. The output from proximity probe is measured in synchronism with rotor mapping in order to determine when the entire surface of the rotor has been mapped - i.e. one complete revolution. The following design specifications of the mini-rotor follows that of a utility-scale rotor:

- Two-pole, 3000 rpm, 50 Hz
- Distributed and concentric field windings
- Shaft-mounted slip rings with static outboard excitation
- Insulated pedestal bearings
- Mono-block milled shaft with slots
- Damper bars

For the presented experimental setup, a wide angle lens ($62^o$ x $49^o$) is used to enable full coverage of the mini-rotor body while maintaining the smallest pixel size possible without compromising the capture of significant details. The mini-rotor body/core is 500 mm in length with a diameter of 180 mm. The field of view of the camera is adjusted to be able to monitor the entire rotor body. This is accomplished by using the proprietary IR camera field of view calculation tool, illustrated in fig. 3. A distance of 440 mm away from the rotor body is calculated to be the optimum field of view by virtue of yielding the following dimensions: the width or horizontal field of view (HFOV) is 527.71 mm, the height or vertical field of view (VFOV) is 396.41 mm and the diagonal or diagonal field of view (DFOV) is 659.52 mm. The instantaneous

Table 1: Constructional details of down-scaled test rotor with large and typical turbo-generator rotor

| Parameter | Test rotor | Turbo-generator rotor |
|---|---|---|
| Number of rotor Slots | 32 | 32 |
| Number of damper bars | 48 | 48 |
| Core diameter | 178.5 mm | 1165 mm |
| Axial length (shaft) | 885 mm | 10990 mm |
| Shaft diameter | 67 mm | 530 mm |

field of view (IFOV) is the geometric dimension of each pixel and is calculated to be 1.38 mm. For optimum measurement results, a 3x3 pixel measurement block known as the MFOV, or recommended smallest measured object size, is suggested by the source [22]. The MFOV is characterised by a group of pixels surrounding a central pixel.

The IR camera is rated at 80 Hz i.e. the ability to capture 80 samples per second. The highest sampling accuracy to map the surface of the rotor is accomplished by operating the rotor at 1 Hz i.e. 80 samples of the rotor body are taken during one revolution. Sampling of the IR camera in actuality is measured to be 77 Hz for the experimental setup. From the determined sampling rate, the optimum measurement pixel configuration is calculated as illustrated in fig. 4. The rotor circumference is 565.5 mm. Dividing this value by the sampling rate produces the required pixel configuration size to map the rotor surface in the radial direction – 7.34 mm. The IFOV is 1.38 mm, thus the number of pixels required in the radial direction is calculated by dividing 7.34 mm by 1.38 mm, yielding 5.31 pixels. Given that only whole pixels are utilised for measurement, 0.31 pixels corresponding to 0.44 mm of the rotor body will not be measured. This will result in approximately 94 % of the rotor body being

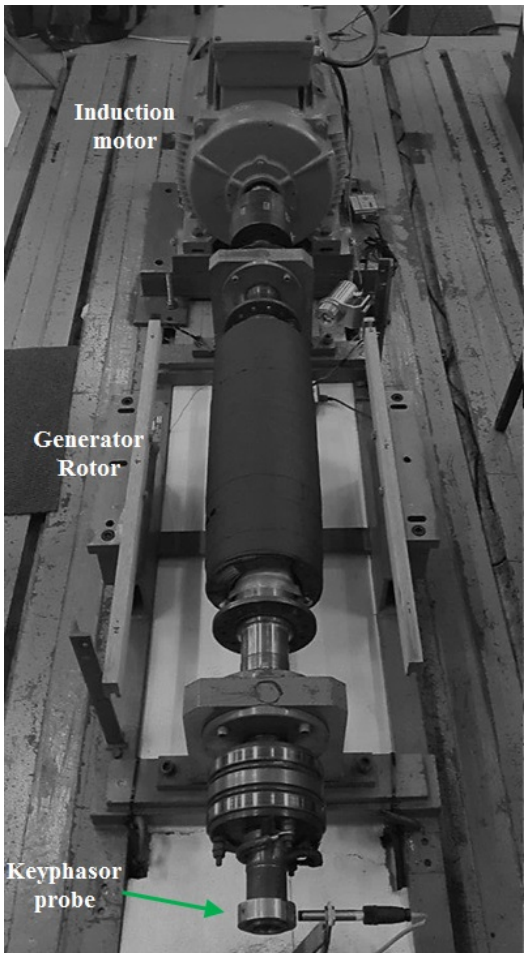


Figure 2: Laboratory setup with mini-rotor used for testing and validation of the thermal mapping technique

mapped in the radial direction. The optimum number of pixels is the radial direction is thus 5 pixels. In the axial direction, the optimal pixel number is chosen as 3, based on achieving a final pixel configuration closest to the optimum of 3x3. Thus, this final pixel configuration is a measuring cluster of 3x5 pixels. This hybrid cluster conforms to the 3x3 optimum measuring configuration as two central pixels are surrounded by adjacent pixels. The number of clusters required to map the rotor surface is calculated at approximately 120 (500 mm divided by 4.14 mm). The area not covered in the axial direction is measured to be 0.78 mm which is considered as negligible as the rotor

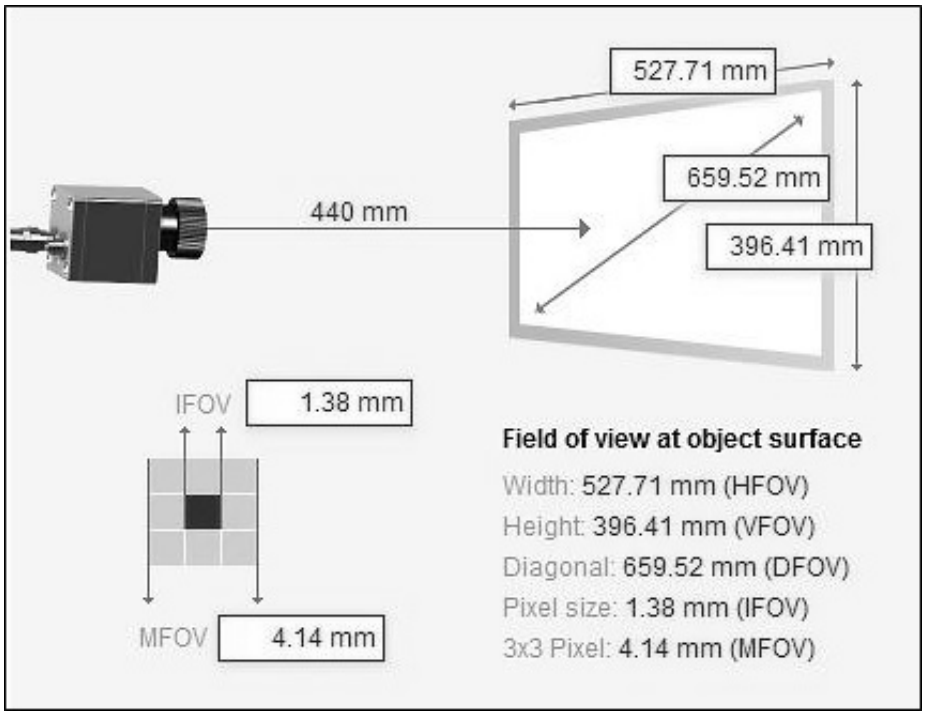


Figure 3: Field of view calculator used to determine camera pixel sample size for mini-rotor

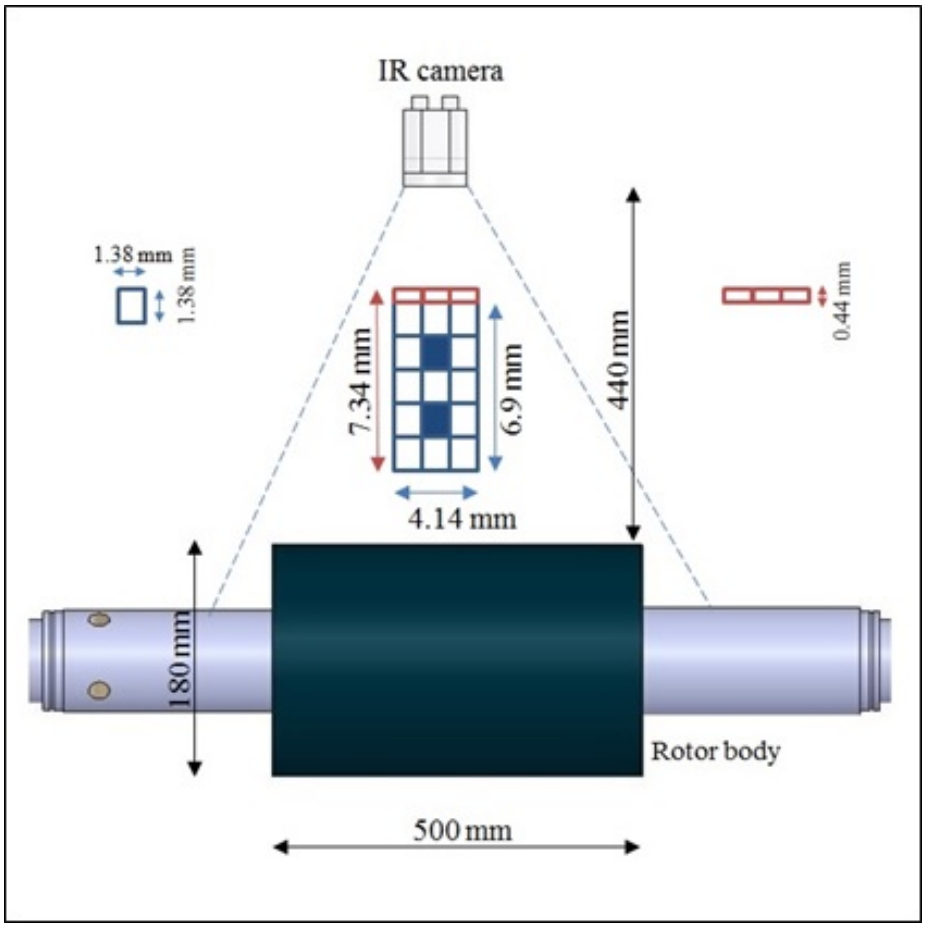


Figure 4: Heat map sampling pixel arrangement base on the field of view of the infrared camera

body covering has an overhang which is larger than the winding - i.e. the configuration is able to map the winding in its entirety, as it is smaller than that rotor body length. Figure 5 illustrates the array used to generate the heat map. The output of the array is a matrix of temperature values that correspond to the rotor body. The data is processed and heat map generation is performed using Matlab. A high-resolution heat map is generated containing a matrix of 120x77 temperature values.

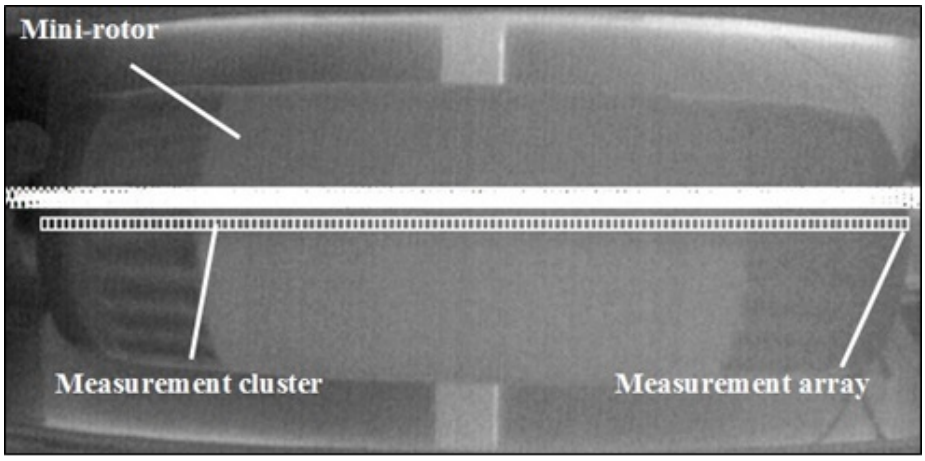


Figure 5: Pixel cluster measurement array used to capture the thermal profile of the mini-rotor surface

## 5. Experimental Validation and Testing of Mapping Method

### *5.1. Methodology*

The presented mapping technique physically maps the surface of the mini-rotor. This method is able to take into consideration the non-uniformities of the mini-rotor construction as opposed to only the idealised design. The salient requirement of the experimental setup is to be able to detail the thermal distribution of the mini-rotor. This is facilitated by the use of a heat map containing temperature values that represent the physical thermal map of the rotor surface. The heat map facilitates the practical assessment of the thermal condition of the rotor and offers the possibility of evaluating acceptance tests such as contemporary TIT methods. Furthermore, the heat map can be interpreted to assist in fault finding. By defining a methodology to scan an array of pixels on the rotor surface and utilising this data to form a matrix of temperature values, it is possible to create a heat map.

The experimental setup is unable to determine the heat distribution within the rotor. This, however, is not the aim of the experimental setup and is not significant owing to the nature of heat diffusion within the rotor body. Heat is diffused from the coils, which are the heat source, to the surrounding components. The surface covering of the rotor (fibre glass banding) is in close contact with coils, making heat diffusion

easily detectable. The direct monitoring of the winding temperature, however, will give some indication as to the internal temperature of the rotor. To all intents and purposes, surface monitoring will practically and adequately determine the thermal distribution of the rotor. Furthermore, the 6 % non-coverage error margin in the radial direction is found to be acceptable, as this does not represent a significant loss of area to prevent the accurate mapping of the rotor surface. The experimental setup is thus validated for the purpose of thermal mapping of the mini-rotor body surface.

In order to validate and test the proposed method, mapping was carried out on the rotor under two different forms of TIT - i.e. FTIT and CTIT, and an inter-turn short-circuit fault on the winding. An enclosure was constructed out of 12 mm fibre board and insulated with a number of layers of Styrofoam to mimic the insulation properties of a full-scale balancing facility. At the drive end of the rotor a face seal is constructed around the bearing housing to enable the shaft to rotate without any loss of air volume/heat within the enclosure. Rubber seals are also utilised at the base of the enclosure. Figure 6 shows the experimental setup used including the IR camera used to perform the thermal mapping. Due to the maximum sampling rate of the camera, the rotational speed of the prime mover is decreased to 60 rpm during the mapping process. After completion of the mapping process the operational speed of 3000 rpm is resumed. In addition to the surface mapping, the winding temperature, enclosure temperature and ambient temperature were recorded.

### *5.2. Results*

FTIT is used to detect instabilities on a turbo-generator rotor under only the influence of air friction/windage while the rotor was operated at 3000 rpm. Therefore, no current excitation is used during this test and heating of the rotor is purely due to friction. For the presented work, this test was performed on the mini-rotor for a total of 8 hours. The ambient temperature was measured at $20^{o}$C, and barometric pressure of 831.3 mb. The thermal map of the recorded surface temperature of the rotor during this test is given in fig. 7. In this map, the x-axis represents the angular position of the rotor, the y-axis represents the axial length of the rotor, and the colour scale corresponds to the surface temperature of the rotor.

It should be highlighted that the specific temperatures in one mapped condition do not necessarily correspond to the same temperatures in a map recorded under different conditions. This intentional formulated in the design of the method as colour resolution is limited and distribution of larger temperature scale of multiple maps will sacrifice resolution a single map. Hence, comparison of different maps should take into consideration the relationship between the specific temperature scale and corresponding colour for a particular test scenario.

The map given in fig. 7 shows uniform heating radially along the surface of the rotor, and a temperature gradient of approximately $4.5^{o}$C along the rotor between the drive and excitation ends of the rotor. The excitation end or non-drive end is at a higher temperature. In practice, this temperature is significant as relatively small differences in temperature can lead to thermal instability. The root cause of this thermal gradient/uneven heating were suspected to be either bearing losses, rub at the non-drive end or slip-ring brush-gear interaction. In order to determine the origin of the temperature gradient, the brush-gear assembly was removed and the test repeated. The ambient temperature measured $21^{o}$C at a barometric pressure of 841.3 mb at the time of FTIT re-testing. The recorded thermal map for the FTIT test without the brush-gear assembly after 8 hours is given in fig. 8. Results indicate that the average surface temperature of the FTIT test without the brush-gear assembly was approximately $23.5^{o}$C lower thereby quantifying the thermal influence of the brush gear.

CTIT is used to detect rotor thermal instability under different levels of current excitation on the windings while operating at 3000 rpm. For the presented investigation, the mini-rotor was excited incrementally at different levels based on the rating of the mini-rotor - i.e. at 5 A, 10 A, 20 A and 35 A. The thermal map recorded after 210 mins under 35 A current excitation is shown in fig. 9. The measured ambient temperature was $21^{o}$C, and barometric pressure 838.9 mb. The frictional effects of the brush-gear assembly interaction are also observed during CTIT as a temperature gradient exists between the drive and non-drive ends of the rotor. The rectangular symmetrical areas of higher temperatures are the pole faces and associated coils on the rotor. The inter-pole areas are represented by the darker spaces on the map.

An inter-turn short-circuit fault on the winding was used to test the fault detection

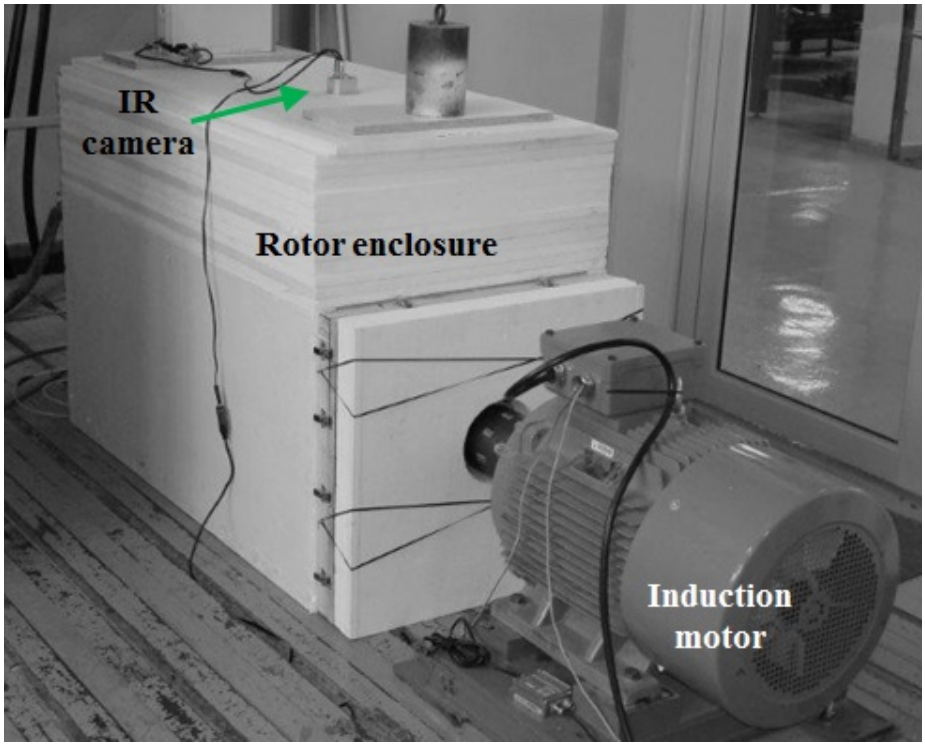


Figure 6: Laboratory setup with thermal-insulation enclosure for mini-rotor and thermal imaging camera.

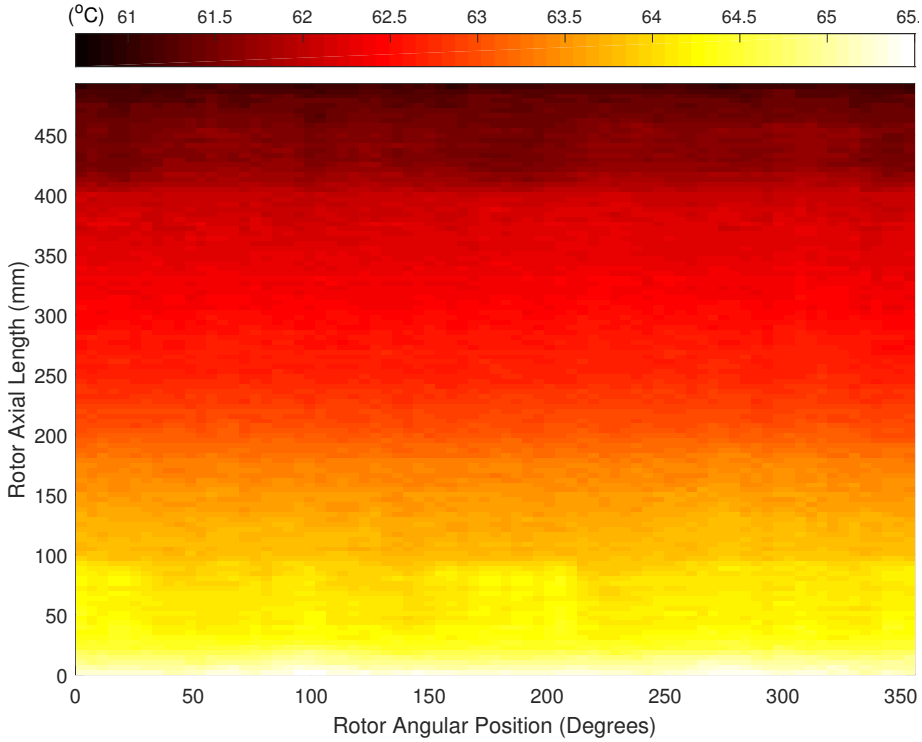


Figure 7: Experimental heat map of down-scaled synchronous generator rotor during friction-only thermal instability test.

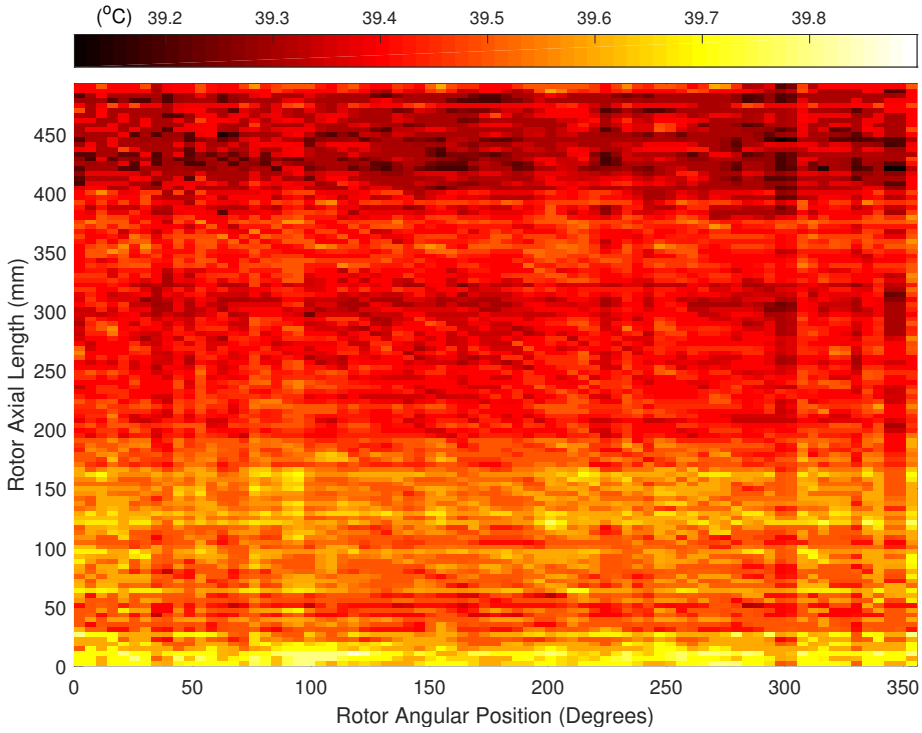


Figure 8: Experimental heat map of down-scaled synchronous generator rotor without brush gear during friction-only thermal instability test.

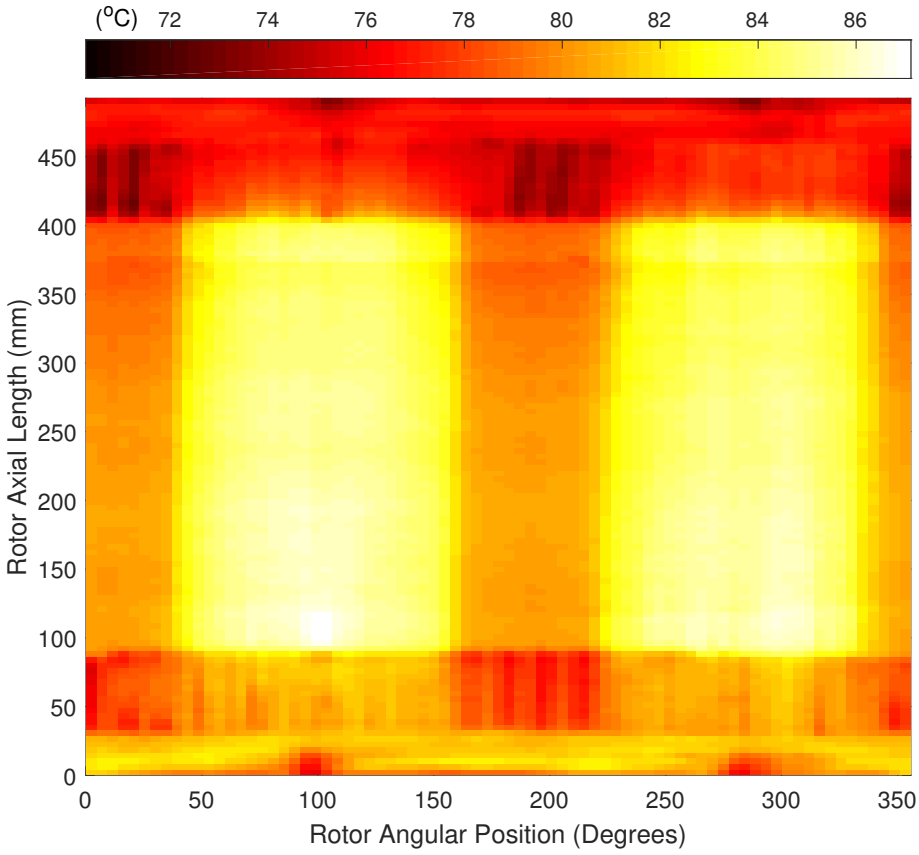


Figure 9: Experimental heat map of down-scaled synchronous generator rotor with current excitation of 30 A after 30 mins.

capability of the present thermal mapping technique. Moreover, this test is used to evaluate the effectiveness of the technique in locating the physical position of the anomaly. An inter-turn short was induced between turns six and seven on coil eight of one pole of the rotor. Current excitation was applied at 15 A to the rotor while operating at 3000 rpm. Figure 10 shows the thermal map of the rotor, under the fault condition, after start-up with no current injected into the windings. Figures 11 and 12 show the thermal maps of the rotor, under the same fault condition, after 30 s and 10 mins, respectively, with 15 A current injected into the windings. These thermal maps show, in a qualitative way, the consistency with which the presented mapping technique indicates the resulting patterns. For instance, in fig. 11, the thermal gradient is observed between the affected area -i.e. approximate angular position of $100^o$ on the non-drive end of the rotor - and the surrounding area of the rotor. However, a similar thermal gradient can still be noticed in the same position in fig. 12, after 10 mins, but at a higher average rotor temperature thereby clearly indicating presence of the fault.

## 6. Discussion

The principle aim of the presented research was to develop an experimental methodology for thermally mapping the surface of a generator rotor. The methodology is yet to be commissioned for mapping the thermal behaviour of a full-scale rotor at a balancing facility. It is required that this technique be initially formulated, implemented under controlled laboratory conditions on a down-scaled rotor, and then validated before implementation on an actual turbo-generator rotor at a high-value plant. However, particular consideration has been given to the specific implications of implementation of the methodology on a full-scale rotor at the local balancing facility.

In the case of a full-scale rotor thermal mapping, initial testing require determination of the precise emissivity of the rotor surface. This can be achieved through first performing calibrated physical temperature measurements and thereafter comparing the results to similar measurements performed using a calibrated laser guided pyrometer. The IR measurement equipment can then be calibrated to match the value of the determined emissivity. One of the significant challenges of performing thermal sensi-

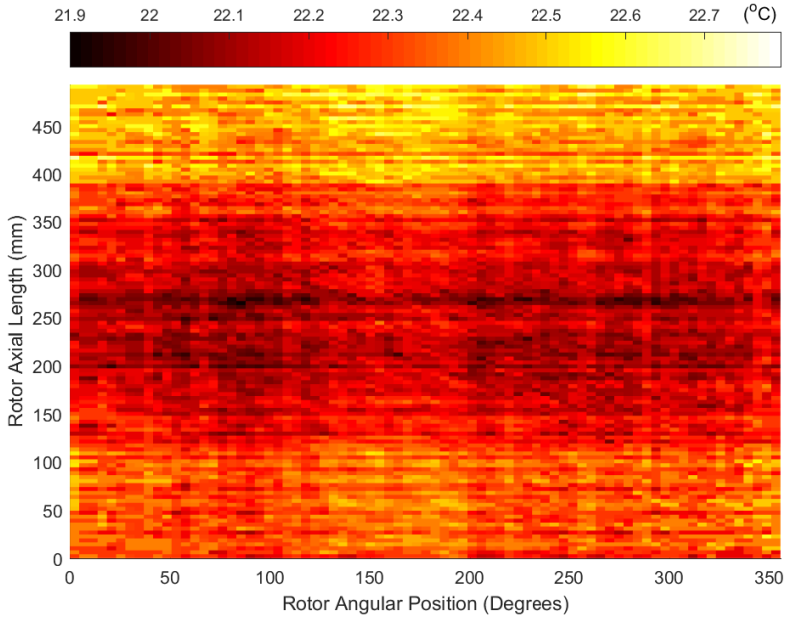


Figure 10: Experimental heat map of down-scaled synchronous generator rotor with inter-turn short-circuit fault and no current excitation.

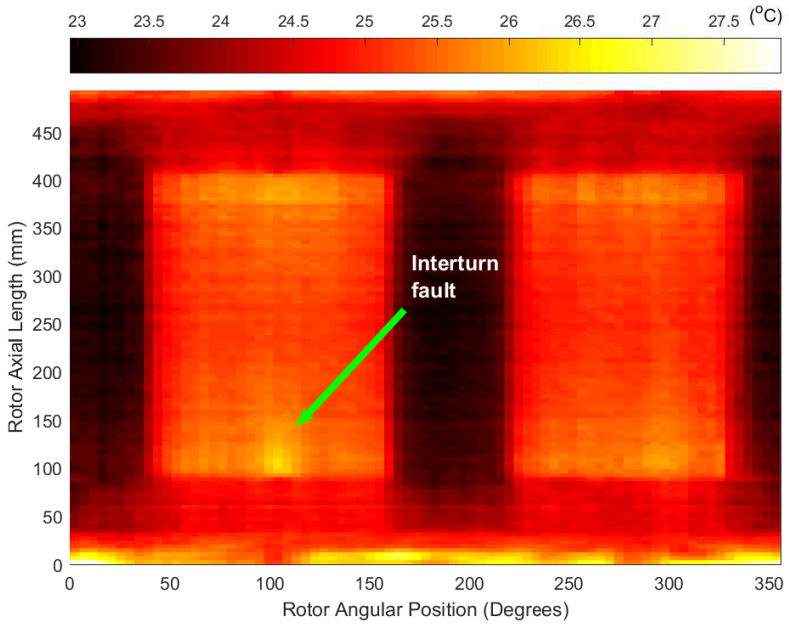


Figure 11: Experimental heat map of down-scaled synchronous generator rotor with inter-turn short-circuit fault and current excitation of 15 A after 30 s.

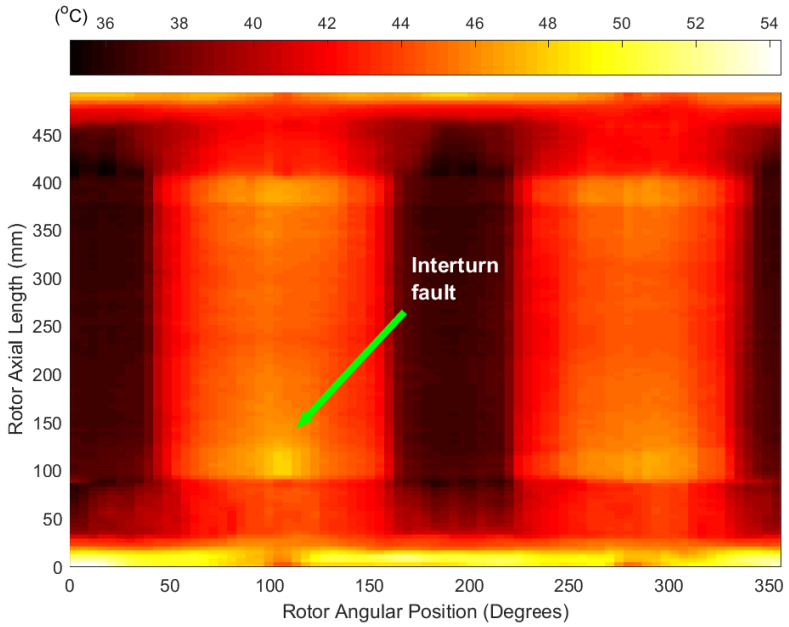


Figure 12: Experimental heat map of down-scaled synchronous generator rotor with inter-turn short-circuit fault and current excitation of 15 A after 10 mins.

tivity tests at full-scale balancing facility is the controlling the effects of the magnetic field generated by the rotor under current excitation. A water-cooled Faraday Cage is typically utilised to contain and limit the effects of the generated fields which may potentially obstruct the field of view of the IR camera used to perform the thermal mapping. This can be overcome by utilizing multiple cameras to perform the mapping as opposed to the single camera used in the presented experimentally-validated test case. Each camera would then observe different sections of the rotor, from outside the cage, in synchronism which would enable a complete thermal map of the rotor surface to constructed by merging the measurement matrices from each camera. Furthermore, the use of multiple cameras, enclosed within cooling jackets to reduce thermal effects, will permit reduction of the cameras distance from the test surface thereby enabling suitable measurement resolution and accurate thermal distribution mapping. It should also be highlighted that a higher or equal resolution mapping on the larger rotor – relative to the resolution achieved with the down-scaled prototype rotor – will not be required as the thermal gradients across the larger rotor surface are not as steep.

Automation of detection of thermal anomalies is also possible through the presented mapping method. The thermal map obtained provides set of temperature-physical coordinates matrices that may be used comparatively against healthy or acceptable tests cases. This will potentially further remove subjective/erroneous analysis by personnel which is present in current instability testing processes. For a full-scale implementation, the development of an automated approach will require extensive baseline thermal mapping of a rotor under varying conditions to formulate an adequate database with which to compare each new test instance.

## 7. Conclusion

Effective acceptance testing of large turbo-generators after maintenance, repair, rewind or manufacture is necessary to determine thermal stability and suitability for service before commissioning. There are a number of tests that are carried out in practice but most of these are component specific tests that do not offer overall assessment of the rotor. Vibration testing is commonly used for this purpose but it does not offer

detection of incipient problems nor does it assist with locating root causes.

The method presented in this paper offers a solution to shortcomings of conventional test techniques as it provides a means of directly mapping surface temperatures to physical coordinates on the rotor. This methodology was validated and tested on a down-scaled turbo-generator rotor in a laboratory setting. Three different test conditions were used - i.e. FTIT and CTIT, and an inter-turn short-circuit fault on the winding. The thermal mapping method shows that the current injection resulted in a heterogeneous distribution of temperatures along the rotor surface as opposed to the homogeneous distribution by FTIT. These maps enabled effective root cause analysis of an existing thermal gradient along the axial length of the rotor. The direct thermal mapping method was also proven to be accurate and timeous in fault detection. The investigated inter-turn fault was located with a high accuracy. Accuracy and practicability offered by the method offers an improved means of troubleshooting a failed acceptance test, which has been found to be difficult when utilising current methods.


[1] M.B. Jevtic, L.Z. Radovanovic and Z.Z. Adamovic, *Numerical and Experimental Aspects of Thermally inducted vibrations in real rotors*, Thermal Science, vol. 15, no. 2, pp. 545-558, 2011.

[2] R.J. Zawaoysky, and W.M. Genovese, *Generator rotor thermal sensitivity – Theory and experience*, GE Reference Library, GER-3809, 2001.

[3] J.G. Paxton, "Turbine generator rotor thermal unbalance", *EPRI Proceedings: Utility Motor and Generator Predictive Maintenance and Refurbishment Conference*, EPRI TR-104625, pp. 112-116, 1994.

[4] A.N. Singh, W.A. Cronje, and W. Doorsamy, "Investigation of thermal instability testing on synchronous generator rotors using an experimental direct mapping method," *In IEEE 26th International Symposium on Industrial Electronics (ISIE)*, pp. 321-328, June 2017.

[5] G. Klempner, and I. Kerszenbaum, *Operation and maintenance of large turbo-generators*, Power Engineering, ed. M.E. El Hawary, John Wiley & Sons, 2004.

[6] M. Sasic, M., B. Lloyd, and A. Elez, ]"Finite element analysis of turbine generator rotor winding shorted turns," *IEEE Transactions on Energy Conversion*, vol. 27, no. 4, p. 930-937, 2012.

[7] B. Irwanto, L. Eckert, and T. Prothmann, "Thermal unbalance behaviour of turbo-generator rotors", *in Proceedings of the 9th IFToMM International Conference on Rotor Dynamics*, Springer, pp. 2231-2242, 2015.

[8] C.V. Maughan, "Impact of generator design on component deterioration mechanisms", *in Iris Rotating Machines Conference*, Schenectady, NY, 2010.

[9] Y. Gao, J. Sun, J. Li, F. Wang, J. Wan, and J. Liu, "Research on Vibration Fault Diagnosis Strategy for Commonly Supported Rotor of Turbogenerator," *IEEE 2nd Information Technology, Networking, Electronic and Automation Control Conference (ITNEC)*, pp. 305-310, 2017.

[10] A. Der Kiureghian, and O. Ditlevsen, *Aleatory or epistemic? Does it matter?*, Structural Safety, vol. 31, no. 2, pp. 105-112, 2009.

[11] E. Smith, "Main generator rotor maintenance - lessons learned", *EPRI*, Palo Alto, California, 2006.

[12] B.M. Weedy, *The determination of the transient temperature distribution in a turboalternator rotor by means of an analogue*, Proceedings of the IEE - Part C: Monographs, vol. 109, no. 15, pp. 126-137, 1962.

[13] J. Han, B. Ge, D. Tao, and W. Li, "Calculation of Temperature Distribution in End Region of Large Turbogenerator Under Different Cooling Mediums," *IEEE Transactions on Industrial Electronics*, no. 2, vol. 65, pp. 1178-1186, 2018.

[14] C.V. Maughan, and J.M. Reschovsky, "Advances in motor and generator rotor health," *in IEEE International Symposium on Electrical Insulation (ISEI)*, 2010.

[15] A. G. Garcia-Ramirez, L. A. Morales-Hernandez, R. A. Osornio-Rios, J. P. Benitez-Rangel, A. Garcia-Perez, and R. de Jesus Romero-Troncoso, "Fault detection in induction motors and the impact on the kinematic chain through thermographic analysis," *Electric Power Systems Research*, 114, pp. 1-9, 2014.

[16] T. Suesut, N. Nunak, T. Nunak, A. Rotrugsa, and Y. Tuppadung, "Emissivity measurements on material and equipment in electrical distribution system," *in 11th International IEEE Conference on Control, Automation and Systems (ICCAS)*, 2011.

[17] E.A.E. Jebaseeli, and S. Paramasivam, *Real-time temperature measurement for the thermal protection of switched reluctance machine*, International Journal of Engineering & Technology, no. 5, pp.0975-4024, 2013.

[18] C. Mejuto, M. Mueller, M. Shanel, A. Mebarki, M. Reekie, and D. Staton, "Improved synchronous machine thermal modelling," *18th International Conference in Electrical Machines*, 2008.

[19] D.P. DeWitt, and G.D. Nutter, *Theory and practice of radiation thermometry*, Wiley 1988.

[20] C.H. Chen, *Generalized association plots: Information visualization via iteratively generated correlation matrices*, Statistica Sinica, vol. 12, no. 1, pp. 7-30, 2002.

[21] L. Wilkinson, and M. Friendly, *The history of the cluster heat map*, The American Statistician, vol. 63, no. 2, 2009.

[22] Micro-Epsilon, *Operators manual thermoIMAGER TIM Connect*, Ortenburg, Germany, 2008.